Mixing of $t\bar{t}$ bound states with the Z boson

Paula J. Franzini and Frederick J. Gilman
Stanford Linear Accelerator Center, Stanford University, Stanford, California 94305
(Received 15 February 1985)

We take seriously the possibility that $t\bar{t}$ bound states are within several GeV/c^2 of the Z-boson mass and make a careful study of this possible near degeneracy using the mass-mixing formalism. Most of the decay width of vector states below the open-top threshold comes from mixing with the Z. In the idealized situation where there is no coupling of the unmixed $t\bar{t}$ state to e^+e^- and $f\bar{f}$, the amplitude for $e^+e^-\to f\bar{f}$ has an exact zero at the unmixed mass. Correspondingly, in the physical situation of nonzero couplings, the cross section for $e^+e^-\to f\bar{f}$ exhibits deep minima. We investigate as well the effects of complex mixing matrix elements above the open-top threshold, and calculate longitudinal polarization and forward-backward asymmetries, where there are large enhancements near $t\bar{t}$ resonance masses.

I. INTRODUCTION

The possibility of mixing between the Z^0 boson and $t\bar{t}$ states has already been discussed in a number of papers.[1-4] Much of this work, guided by theoretical speculation on the top-quark mass m_t, was concerned with the situation where the Z mass was much higher than $2m_t$. However, the discovery[5] of the Z^0 at CERN, and the more recent evidence[6] for a top quark with a mass between 30 and 50 GeV suggest that the scenario where there is a near degeneracy in mass between $t\bar{t}$ states and the Z merits a closer and more careful look.[7]

In the next section we set up the mass-mixing formalism needed to study this problem. We then proceed to study the mixing of one vector ($J^{PC}=1^{--}$) $t\bar{t}$ state V with the Z, solving the problem analytically and studying various limiting cases. There is an exact zero in the amplitude for $e^+e^-\to f\bar{f}$ at the bare (unmixed) mass of the V when the couplings of the bare V state to both e^+e^- and $f\bar{f}$ are zero. We set out the formulas for the couplings, cross sections, asymmetries, etc., and then consider the corrections of allowing nonzero couplings and of including $e^+e^-\to\gamma\to f\bar{f}$. For $\sigma(e^+e^-\to f\bar{f})$ these have a small effect on the overall shape, which still has a strong minimum, whose position is slightly shifted. For the polarization and front-back asymmetries the effects are much more dramatic. The section concludes with the formalism needed for mixing the Z with an arbitrary number of vector $t\bar{t}$ states, both below and above the open-top threshold, where the off-diagonal mass-mixing matrix element becomes complex.

In Sec. III we briefly discuss heavy-quark potentials and the spectrum of $t\bar{t}$ states which results. We use the potential of Richardson[8] and find roughly 13 S states below the open-top threshold. Section IV then contains the results following from applying the mixing formalism in Sec. II to the Z and the set of $t\bar{t}$ states described in Sec. III. We consider $\sigma(e^+e^-\to f\bar{f})$ in situations where $2m_t$ is less than, roughly equal to, and greater than M_z. There are striking interference patterns observed in $\sigma(e^+e^-\to f\bar{f})$ as well as in the longitudinal and front-back asymmetries. We conclude with a sobering look at what the experimentally unavoidable spread in beam energies does to these interference patterns.

II. MIXING

As we are considering mixing between states in a limited energy range far from threshold we may safely use the mass-mixing formalism.[9,10] If we take the simplified case of only two states, the Z and one vector ($J^{PC}=1^{--}$) $t\bar{t}$ resonance V then the 2×2 mass matrix has the form

$$\mathcal{M}_0^2=\begin{bmatrix} M_{V_0}^2-i\Gamma_{V_0}M_{V_0} & \delta m^2 \\ \delta m^2 & M_{Z_0}^2-i\Gamma_{Z_0}M_{Z_0}\end{bmatrix}, \tag{2.1}$$

and the matrix propagator,

$$\mathcal{D}(s)=\frac{1}{\mathcal{M}_0^2-s\,\mathbf{1}}\ . \tag{2.2}$$

Here $\mathcal{M}_0^2$ is the (undiagonalized) mass matrix with elements expressed in terms of "bare" masses (M_{Z_0} and M_{V_0}) and widths (Γ_{Z_0} and Γ_{V_0}). Within the spirit of the mass-mixing formalism we take the initial widths to be constants, with no explicit functional dependence on mass.[9] Inclusion of such a mass dependence, or working with the mass rather than mass-squared matrix, results in amplitude changes of a few percent in the limited mass range within which we are working.

The off-diagonal term δm^2, which induces the mixing, originates in the (vector) coupling of the Z to the t quark contained in the $t\bar{t}$ bound state (see Fig. 1). Its value is

$$\begin{aligned}\delta m^2&=2\sqrt{3}\,|\psi(0)|\sqrt{M_{V_0}}g_{V,t}\\ &=2\sqrt{3}\,|\psi(0)|\sqrt{M_{V_0}}\left[\frac{e(1-\frac{8}{3}\sin^2\theta_W)}{4\sin\theta_W\cos\theta_W}\right],\end{aligned} \tag{2.3}$$

where $\psi(0)$ is the wave function of the $t\bar{t}$ bound state at the origin and θ_W is the weak mixing angle (so that[11] $\sin^2\theta_W\approx 0.22$). The factor of $\sqrt{3}$ arises from color.

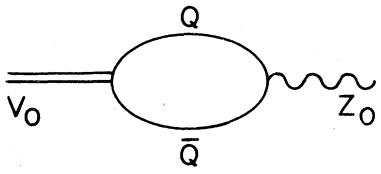

FIG. 1. Diagrammatic representation of the process causing Z_0-V_0 mixing.

For the P states δm^2 is proportional to the derivative of the wave function at the origin, with concomitant much smaller mixing (by roughly an order of magnitude for $t\bar{t}$). This is examined in detail in Ref. 7.

For purposes of calculation one can work with the mass matrix in this nondiagonal basis, sandwiching the propagator in Eq. (2.2) between initial and final spinors which express the coupling strength of the "bare" V_0 and Z_0 to the initial and final states, respectively. For some purposes, however, it is more useful to go to the diagonal basis, obtaining along the way the physical states and eigenvalues. For this purpose we rewrite Eq. (2.1) as

$$\mathcal{M}_0^2=\tfrac{1}{2}(M_{V_0}^2-iM_{V_0}\Gamma_{V_0}+M_{Z_0}^2-iM_{Z_0}\Gamma_{Z_0})\mathbf{1}+\Delta^2\hat{\mathbf{n}}\cdot\boldsymbol{\sigma}\ , \tag{2.4}$$

where

$$\Delta^2=[(M_{V_0}^2-iM_{V_0}\Gamma_{V_0}-M_{Z_0}^2+iM_{Z_0}\Gamma_{Z_0})^2/4+(\delta m^2)^2]^{1/2}\ , \tag{2.5a}$$

$$\hat{\mathbf{n}}=\cos\theta\,\hat{\mathbf{z}}+\sin\theta\,\hat{\mathbf{x}}\ , \tag{2.5b}$$

and the complex angle θ is given by

$$\sin\theta=\delta m^2/\Delta^2\ . \tag{2.5c}$$

It is then easy to see that $\mathcal{R}\mathcal{M}_0^2\mathcal{R}^{-1}$, where $\mathcal{R}=e^{(i\theta/2)\sigma_y}$, is diagonal, with eigenvalues

$$M_V^2-iM_V\Gamma_V=\tfrac{1}{2}(M_{V_0}^2-i\Gamma_{V_0}M_{V_0}+M_{Z_0}^2-i\Gamma_{Z_0}M_{Z_0})+\Delta^2\ , \tag{2.6a}$$

$$M_Z^2-iM_Z\Gamma_Z=\tfrac{1}{2}(M_{V_0}^2-i\Gamma_{V_0}M_{V_0}+M_{Z_0}^2-i\Gamma_{Z_0}M_{Z_0})-\Delta^2\ , \tag{2.6b}$$

and that the physical eigenstates are

$$|V\rangle=e^{-i(\theta/2)\sigma_y}\begin{bmatrix}1\\0\end{bmatrix}=\cos\frac{\theta}{2}\,|V_0\rangle-\sin\frac{\theta}{2}\,|Z_0\rangle\ , \tag{2.7}$$

$$|Z\rangle=e^{i(\theta/2)\sigma_y}\begin{bmatrix}0\\1\end{bmatrix}=\sin\frac{\theta}{2}\,|V_0\rangle+\cos\frac{\theta}{2}\,|Z_0\rangle\ .$$

Since θ is generally complex, R is symmetric but not unitary.

When the narrow state V is far from the Z, these results simplify, and the mixing is characterized by

$$\tfrac{1}{2}\sin\theta\approx\frac{\theta}{2}\approx\frac{\delta m^2}{M_{V_0}^2-M_{Z_0}^2+iM_{Z_0}\Gamma_{Z_0}}\ . \tag{2.8}$$

As the magnitude of the right-hand side turns out to be (see below) $\lesssim 0.1$ even when $M_{V_0}=M_{Z_0}$, this is even a good approximation when the V and Z are close. The small admixture of the V_0 in the Z has a totally negligible effect, while the corresponding small Z_0 admixture to the V has relatively large effects because of the much larger Z_0 couplings to fermion-antifermion pairs. Alternatively, when the mixing is small, the problem of V decays involving the Z can be treated directly by explicitly calculating diagrams involving an intermediate Z, with identical results[2] to those obtained using Eq. (2.8).

Now let us consider the situation of interest to us when the state V_0 is near the Z_0 and most of the width of the V comes, as we shall see, from mixing with the Z. It is useful to consider then the idealized case where the unmixed state V_0 has no coupling to particular initial and final states, e.g., e^+e^- and $\mu^+\mu^-$. From Eq. (2.7) we see that in this case the couplings of the physical V and Z to the initial and final states are

$$g_V=-\sin\frac{\theta}{2}g_{Z_0},\quad g_Z=\cos\frac{\theta}{2}g_{Z_0}\ . \tag{2.9}$$

Consequently, the scattering amplitude

$$A_{fi}(s)=\frac{g_{Vf}g_{Vi}}{M_V^2-iM_V\Gamma_V-s}+\frac{g_{Zf}g_{Zi}}{M_Z^2-iM_Z\Gamma_Z-s} \tag{2.10}$$

simplifies to

$$A_{fi}(s)=g_{Z_0f}g_{Z_0i}\left[\frac{\sin^2(\theta/2)}{M_V^2-iM_V\Gamma_V-s}+\frac{\cos^2(\theta/2)}{M_Z^2-iM_Z\Gamma_Z-s}\right]\ . \tag{2.11}$$

At the point $s=M_{V_0}^2-iM_{V_0}\Gamma_{V_0}$, the (complex) mass squared of the unmixed $t\bar{t}$ state,

$$A_{fi}(M_{V_0}^2-iM_{V_0}\Gamma_{V_0})=g_{Z_0f}g_{Z_0i}\left[\frac{\sin^2(\theta/2)}{\Delta^2(\cos\theta-1)}+\frac{\cos^2(\theta/2)}{\Delta^2(\cos\theta+1)}\right]=0\ , \tag{2.12}$$

when we use the relationship in Eqs. (2.6a) and (2.6b) between the "dressed" masses and "bare" masses together with the definition of θ in Eq. (2.5c). Therefore, there is an exact zero of the amplitude $A_{fi}(s)$ at the position of the unmixed V_0 mass when the unmixed state does not couple to either the initial or final state.[12]

How close is the actual situation to this idealized one? To answer this we need to put in some numerical values and insert couplings from the standard model. From the Richardson[8] potential discussed in the next section we take $|\psi(0)|^2\approx 65$ GeV^3 for the $1S$ vector-meson $t\bar{t}$ ground state when the top-quark mass is such that $M_{V_0}\approx M_Z$ (which we take as[11,13] 93 GeV). According to Eq. (2.3), we then have

$$\delta m^2=20\ \text{GeV}^2 \tag{2.13}$$

for mixing of the $1S$ state with the Z_0.

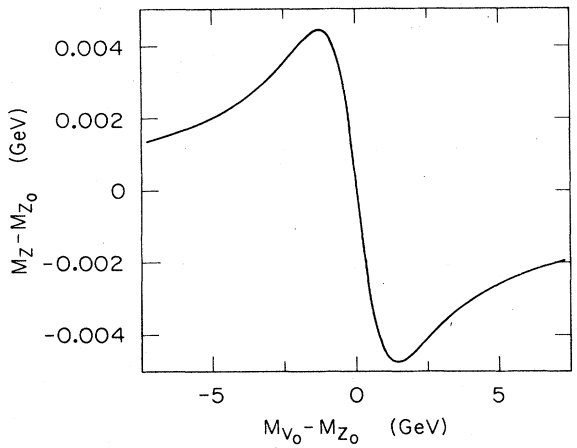

FIG. 2. Change in the mass of the physical Z state due to mixing with the $t\bar{t}$ ground state as a function of the mass difference of the bare states (M_{Z_0} is held fixed at 93 GeV, while M_{V_0} is varied).

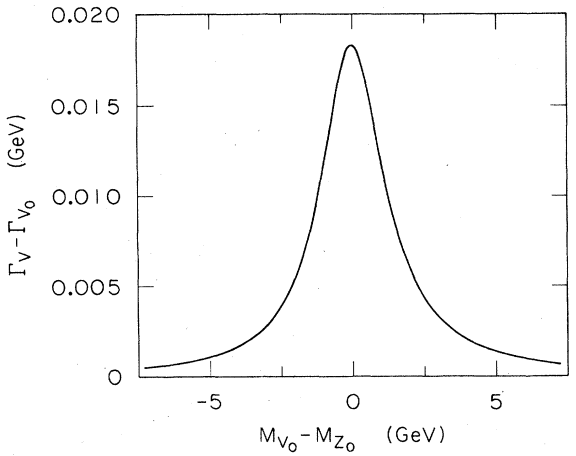

FIG. 3. Change in the width of the physical $t\bar{t}$ ground state V, as a function of the mass difference of the bare states (M_{Z_0} is held fixed at 93 GeV, while M_{V_0} is varied).

Preservation of the trace of the mass matrix under diagonalization implies that $M_V{}^2 - M_{V_0}{}^2 = -(M_Z{}^2 - M_{Z_0}{}^2)$, so the squared masses are shifted equally and oppositely, and similarly for widths. We solve Eqs. (2.6) for the "dressed" masses and widths as a function of M_{V_0}, taking $M_{Z_0} = 93$ GeV and $\Gamma_{Z_0} = 2.7$ GeV [$\Gamma_{V_0} \sim 100$ keV (Ref. 14) and can be neglected at this stage of the calculation], with the results shown in Figs. 2 and 3. The mass shift, at most about 4 MeV (i.e., $\Delta M/M \lesssim 5\times 10^{-5}$), is negligible. On the other hand, V does acquire a sizable width which is maximal when the V_0 and Z_0 coincide, at which point

$$\Gamma_V \approx \frac{(\delta m^2)^2}{M_{Z_0}{}^2 \Gamma_{Z_0}} \approx 18 \text{ MeV} , \tag{2.14}$$

i.e., more than two orders of magnitude greater than the bare width.

The calculation of the cross section, as well as the polarization and front-back asymmetries, is expedited by considering Feynman amplitudes A_{fi} for initial and final fermions of definite handedness, which are in principle separately measurable and hence do not interfere (since the interactions are mixtures of V and A the corresponding antifermions are forced to have opposite handedness). The couplings of the gauge bosons to fermions of charge Qe and third component of weak isopin T_{3L} are given in the standard model as

$$\begin{aligned} g_{Z_0,L} &= e\frac{T_{3L} - Q\sin^2\theta_W}{\sin\theta_W \cos\theta_W} , \\ g_{Z_0,R} &= e\frac{-Q\sin^2\theta_W}{\sin\theta_W\cos\theta_W} , \\ g_{\gamma,L} &= g_{\gamma,R} = eQ , \end{aligned} \tag{2.15}$$

while that induced by an intermediate virtual photon for the V_0 is

$$g_{V_0,L} = g_{V_0,R} = \tfrac{4}{3} e^2 Q \sqrt{3} (M_{V_0})^{-3/2} |\psi(0)| . \tag{2.16}$$

The angular dependence of the various amplitudes is given by standard arguments, so that the unpolarized cross section is

$$\begin{aligned} \frac{d\sigma(s,\theta)}{d\cos\theta} = \frac{s}{32\pi} \Bigg[& |A_{L,L}(s)|^2 \left[\frac{1+\cos\theta}{2}\right]^2 + |A_{L,R}(s)|^2 \left[\frac{1-\cos\theta}{2}\right]^2 \\ & + |A_{R,L}(s)|^2 \left[\frac{1-\cos\theta}{2}\right]^2 + |A_{R,R}(s)|^2 \left[\frac{1+\cos\theta}{2}\right]^2 \Bigg] . \end{aligned} \tag{2.17}$$

Recalling $\sigma_{pt}(s) = 4\pi\alpha^2/3s$,

$$R(s) = \frac{\sigma(s)}{\sigma_{pt}(s)} = \frac{s^2}{64\pi^2\alpha^2} [\,|A_{L,L}(s)|^2 + |A_{L,R}(s)|^2 + |A_{R,L}(s)|^2 + |A_{R,R}(s)|^2\,] . \tag{2.18}$$

The value of R for $e^+e^- \to \mu^+\mu^-$ in the situation where M_{V_0} is 1 GeV below M_Z, which we arbitrarily choose for the purposes of illustration, is shown in Fig. 4. The dotted curve is with the Z alone, while the dashed curve shows the case in which the couplings of the V_0 to initial and final fermions are set to zero. We find in this latter case that

$$R = \frac{(|g_{Z_0,L}|^2 + |g_{Z_0,R}|^2)_i (|g_{Z_0,L}|^2 + |g_{Z_0,R}|^2)_f}{64\pi^2\alpha^2} \left| \frac{s(s - M_{V_0}{}^2 + i\Gamma_{V_0} M_{V_0})}{(s - M_{V_0}{}^2 + i\Gamma_{V_0} M_{V_0})(s - M_{Z_0}{}^2 + i\Gamma_{Z_0} M_{Z_0}) - (\delta m^2)^2} \right|^2 . \tag{2.19}$$

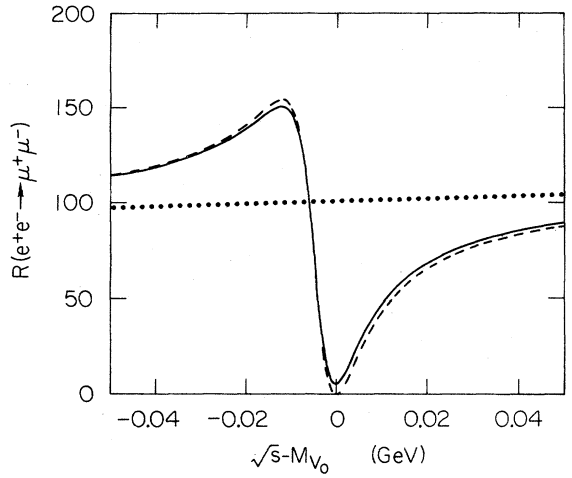

FIG. 4. $R(e^+e^-\to\mu^+\mu^-)$ arising through the Z alone (dotted curve), through Z and V but no coupling of V_0 to the initial or final states (dashed curve), and from Z, V, and γ including bare V_0 couplings (solid curve). The V_0 state has a total width of 100 keV, and mass of 92 GeV.

Here we have done the calculation in the unmixed basis, where it is easier. As demanded by Eq. (2.12), there is an exact zero of the amplitude at a value of s equal to the (complex) bare mass squared of the V_0. While not visible in Fig. 4, the dashed curve does not precisely go through zero, but to $R\approx 5\times 10^{-3}$, since we have made $\Gamma_{V_0}=100$ keV and the zero of the amplitude is slightly off the real energy axis. The realistic case, including the photon intermediate state and bare V_0 couplings as per Eq. (2.16), is shown by the solid line. There still is a deep dip near M_{V_0}. A similar dip occurs for all the $^3S_1$ states below open-top threshold, except that the effect occurs over a narrower energy region for the higher states since their widths (acquired mostly from mixing) are smaller. When $M_{V_0}>M_{Z_0}$ the dip occurs before the peak, rather than after it as in Fig. 4. For the very fortuitous case where $M_{V_0}=M_{Z_0}$, there is no peak at all; only a near zero right in the middle of the Z. Similar behavior is exhibited for $e^+e^-\to u\bar{u}$ and $e^+e^-\to d\bar{d}$.

Since we have the cross section in terms of amplitudes for fermions of definite handedness it is easy to find the expression for the longitudinal polarization (of the initial e^-) asymmetry:

$$A_{\rm POL}(s,\theta)=\frac{A_1(s)+[2\cos\theta/(1+\cos^2\theta)]A_2(s)}{1+[2\cos\theta/(1+\cos^2\theta)]A_{\rm FB}(s)}\ , \qquad (2.20)$$

where

$$A_1=\frac{|A_{R,R}|^2+|A_{L,R}|^2-|A_{R,L}|^2-|A_{L,L}|^2}{|A_{R,R}|^2+|A_{L,R}|^2+|A_{R,L}|^2+|A_{L,L}|^2}\ ,$$
$$A_2=\frac{|A_{R,R}|^2+|A_{R,L}|^2-|A_{L,R}|^2-|A_{L,L}|^2}{|A_{R,R}|^2+|A_{L,R}|^2+|A_{R,L}|^2+|A_{L,L}|^2} \qquad (2.21)$$

and the front-back asymmetry

$$A_{\rm FB}=\frac{|A_{R,R}|^2+|A_{L,L}|^2-|A_{L,R}|^2-|A_{R,L}|^2}{|A_{R,R}|^2+|A_{L,R}|^2+|A_{R,L}|^2+|A_{L,L}|^2}\ . \qquad (2.22)$$

(The quantity $A_{\rm FB}$ used here has a maximum magnitude of unity. The more usual front-back asymmetry obtained by integrating over the forward and backward hemispheres is a factor of $\frac{3}{4}$ smaller.) If we pay no attention to the angular distribution of the final-state fermions and integrate over the center-of-mass scattering angle θ, then we are only sensitive to $A_1(s)$, which is sometimes referred to as "the" polarization asymmetry. For $e^+e^-\to\mu^+\mu^-$, $A_1(s)=A_2(s)$ and there is no distinction between them anyway. Figure 5 displays the polarization asymmetry for the reaction $e^+e^-\to\mu^+\mu^-$ when M_{V_0} is 1 GeV less than M_{Z_0}. Again the dashed curve gives the result when the bare V_0 has no coupling to the initial or final fermions. Since in this case the coupling of V to the initial and final fermions comes entirely through mixing with the Z_0, the ratios of its helicity couplings are identi-

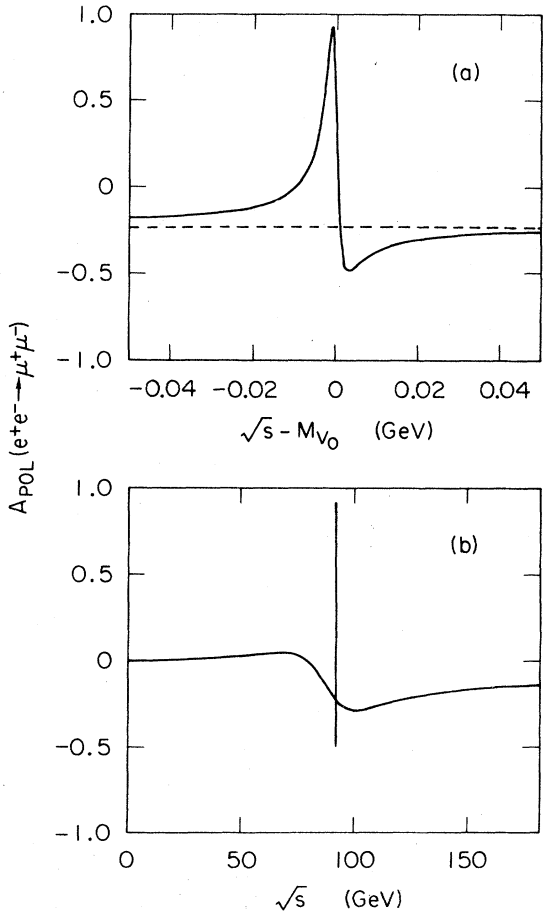

FIG. 5. Polarization asymmetry with the $t\bar{t}$ ground state 1 GeV/c^2 below the Z ($M_{V_0}=92$ GeV/c^2). The polarization asymmetry is shown with all effects considered (solid curve), and additionally in the more detailed figure, $A_{\rm POL}$ for the Z alone is shown (dashed curve).

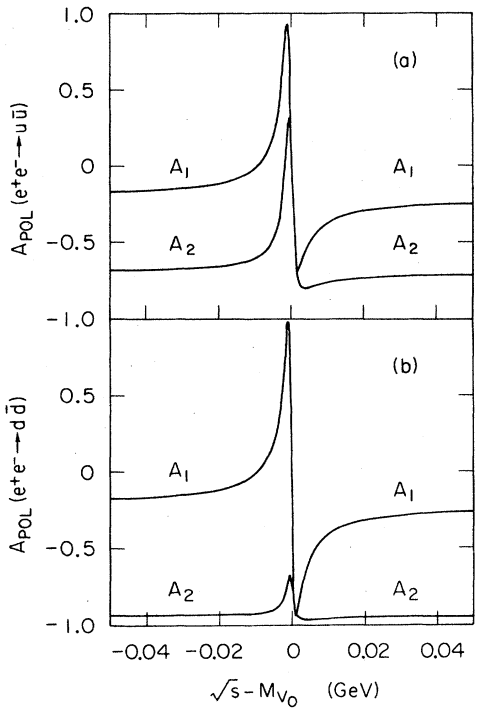

FIG. 6. The two polarization-asymmetry components, A_1 and A_2, for $e^+e^-\to u\bar{u}$ and $e^+e^-\to d\bar{d}$ in the vicinity of the $t\bar{t}$ ground state when $M_{V_0}=92$ GeV/c^2.

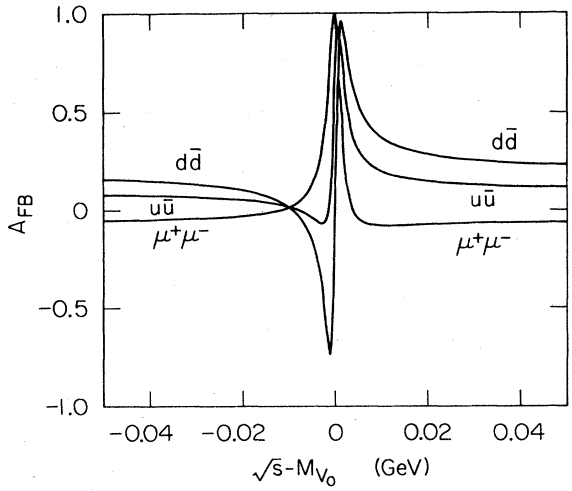

FIG. 7. The forward-backward asymmetry for $e^+e^-\to\mu^+\mu^-$, $e^+e^-\to u\bar{u}$, and $e^+e^-\to d\bar{d}$ in the vicinity of the $t\bar{t}$ ground state when $M_{V_0}=92$ GeV/c^2.

cal to those of the Z and the value of $A_{\rm POL}$ is identical to that for the Z alone. However, when the amplitudes involving virtual photons are included (solid curve in Fig. 5), the effects are dramatic. Although the amplitudes involving virtual photons are small, those coming from $V+Z$ also are small near M_{V_0} and one sees a large effect characteristic of the interference of the real part of the Breit-Wigner amplitude of the V with the rest of the amplitude.

Figure 6 shows the polarization asymmetries A_1 and A_2 in the vicinity of M_{V_0} for production of charge $2e/3$ and $-e/3$ quarks, u and d. Again one observes characteristic interference patterns due to the real part (e.g., in A_1 for $u\bar{u}$) and/or imaginary part (e.g., in A_2 for $d\bar{d}$) of the Breit-Wigner resonance amplitude of the V interfering with the rest of the amplitude due to $\gamma+Z$. The quark production amplitudes used in this computation do not include the contributions from strong interactions, i.e., $V\to$intermediate gluons$\to q\bar{q}$, which could in principle contribute further coherently interfering amplitudes, modifying the interference patterns. Similar comments hold for the forward-backward asymmetry shown in Fig. 7 for $\sqrt{s}$ in the neighborhood of M_{V_0}. As the asymmetries for $\gamma+Z$ alone do not vary strongly over the width of the Z, the general form of the asymmetry after the state V is introduced does not depend strongly on whether it is a few GeV below or above the Z mass.

The extension of the formalism to encompass mixing of the Z with an arbitrary number of $t\bar{t}$ states is straightforward. For n states the mass matrix is $(n+1)\times(n+1)$:

$$\mathcal{M}_0^2=\begin{pmatrix} M_{Z_0}^2-iM_{Z_0}\Gamma_{Z_0} & \delta m^2 & \delta m'^2 & \cdots \\ \delta m^2 & M_{V_0}^2-iM_{V_0}\Gamma_{V_0} & 0 & 0 \\ \delta m'^2 & 0 & M_{V_0'}^2-iM_{V_0'}\Gamma_{V_0'} & 0 \\ \vdots & 0 & 0 & \ddots \end{pmatrix}, \tag{2.23}$$

where $\delta m^2,\delta m'^2,\ldots$ parametrize the mixing between the Z and the spectrum of $t\bar{t}$ states $V,V',\ldots$. Mixing directly (e.g., through an intermediate photon) between $t\bar{t}$ states is very small and has been neglected.

If one works only to second order in $\delta m^2,\delta m'^2,\ldots$ then it is possible to write a simple expression for the rotation that diagonalizes M_0^2 and hence its eigenvalues and eigenvectors. We have found numerically that this gives a fair approximation to the masses and widths of the dressed states $V,V',\ldots$, and a good approximation to the cross sections. In our subsequent work we calculate in the unmixed basis, as the matrix can be inverted exactly. While this can be done analytically, it is easier to carry out the matrix manipulations numerically at each value of s.

Finally, above the open-top threshold two interesting

effects occur. The bare width of the $t\bar{t}$ states will no longer be negligible, changing the near zeros in cross sections to minima where the cross section drops by less than an order of magnitude. Further, the mixing term δm^2 picks up an imaginary part as physical intermediate states are allowed ($V_0 \to T_i \bar{T}_i \to Z_0$), giving

$$\mathrm{Im}\delta m^2 = -\sum_i (M_{Z_0}\Gamma_{Z_0\to T_i\bar{T}_i})^{1/2}(M_{V_0}\Gamma_{V_0\to T_i\bar{T}_i})^{1/2} , \tag{2.24}$$

where the sum extends over all physical intermediate states. In principle the imaginary part of δm^2 can be comparable to the real part, causing sizable changes in the interference.

III. $t\bar{t}$ STATES AND THRESHOLDS

We shall be utilizing the spectrum of $t\bar{t}$ states and their wave functions determined using the heavy-quark potential of Richardson.[8] It has the advantages of correct long- and short-range behavior together with a minimal number of parameters. In addition, it provides a very good set of predictions for the $^3S_1$ states of the Υ system.[15] This potential is specified in momentum space by

$$\tilde{V}(q^2) = -\frac{4}{3}\frac{12\pi}{33-2n_f}\frac{1}{q^2\ln(1+q^2/\Lambda^2)} . \tag{3.1}$$

We use $n_f=3$, since the relevant energy scale is the momentum of the bound quarks, which is less than, or around, the mass of the charm quark; furthermore, as this is a phenomenological potential, we wish to use the same parameters as did Richardson. It can be rewritten in position space as

$$V(r) = \frac{8\pi}{33-2n_f}\Lambda\left[\Lambda r - \frac{f(\Lambda r)}{\Lambda r}\right] , \tag{3.2}$$

where

$$f(t) = \left[1 - 4\int_1^\infty \frac{dq}{q}\frac{e^{-qt}}{[\ln(q^2-1)]^2+\pi^2}\right] . \tag{3.3}$$

We evaluate this potential numerically using[8] $\Lambda=0.398$ GeV, and then solve the radial Schrödinger equation,

$$u'' + \frac{2(l+1)}{r}u' + \frac{2\mu}{\hbar^2}[E - V(r)]u = 0 , \tag{3.4}$$

where l is the angular momentum and $u(r)r^l = R(r)$, the radial wave function. The first several energy levels, as a function of the top-quark mass m_t, are shown in Fig. 8 (see Ref. 16). The corresponding values of $\psi(0) = R(0)/\sqrt{4\pi}$, the wave function at the origin for the S states, are shown in Fig. 9. These wave functions are normalized with the condition

$$4\pi\int |\psi(r)|^2 r^2 dr = 1 . \tag{3.5}$$

With this normalization the leptonic width (through an intermediate photon) is[17,18]

$$\Gamma(V_0 \to e^+e^-) = \frac{16\pi\alpha^2}{M_{V_0}^2}|\psi(0)|^2 Q_t^2 , \tag{3.6}$$

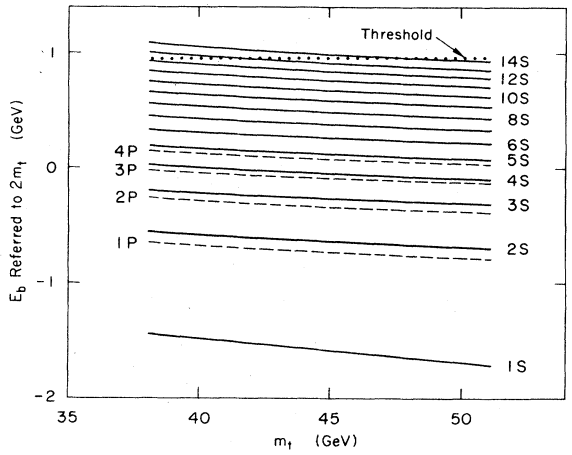

FIG. 8. Binding energy of the S and P $t\bar{t}$ states versus m_t, where $m(t\bar{t}) = 2m_t + E_B$. The heavy line at 0.95 GeV is the threshold for open-top production relative to $2m_t$, which has a very weak dependence on m_t, for such large values of m_t (see text).

and corresponds to a leptonic width of about 9 keV for the ground state.

To calculate where the threshold for bare-top production occurs, we basically follow Eichten and Gottfried.[19] If we use the charm quark as a baseline we have

$$m_T - m_t = m_D - m_c + \tfrac{3}{4}(1 - m_c/m_t)\delta_c , \tag{3.7}$$

where the last term corrects for the hyperfine splitting between the D^* and D and between the T^* and T (the quantity $\delta_c = m_{D^*} - m_D = 0.141$ GeV). Inserting the mass of the charm quark appropriate to the Richardson potential (1.491 GeV), and the experimental D mass, yields $m_T - m_t = 0.477$ GeV. Alternately, we may use the bottom system as a baseline:

$$m_T - m_t = m_B - m_b + \tfrac{3}{4}(1 - m_b/m_t)\delta_b , \tag{3.8}$$

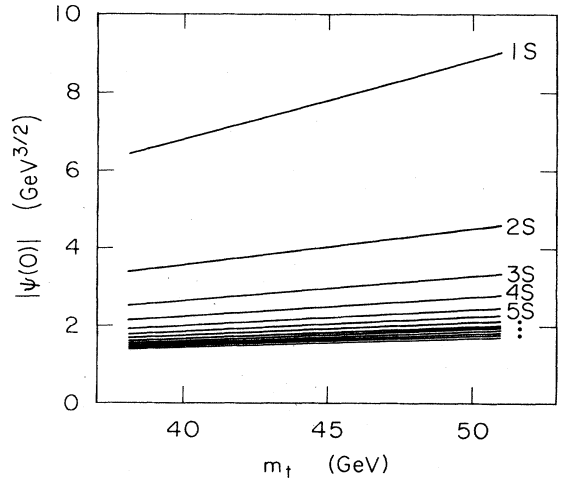

FIG. 9. Wave function at the origin, from the Richardson potential, for the S $t\bar{t}$ states, versus m_t.

where now[20] $\delta_b = m_{B^*} - m_B = 0.052$ GeV. Again, inserting the quark mass appropriate to the Richardson potential ($m_b = 4.883$ GeV), we find $m_T - m_t = 0.425$ GeV.

The threshold is found at $2m_T$, i.e., 0.95 GeV $+2m_t$ or 0.85 GeV $+2m_t$ from Eq. (3.7) or (3.8), respectively. In Fig. 8 we have taken it to be at 0.95 GeV$+2m_t$ (indicated by the solid line), with the result that there are 13 $^3S_1$ states below open-top threshold for $m_t \approx 45$ GeV. Since the level spacing is about one $^3S_1$ state per hundred MeV near threshold, we would lose one such state to the continuum if we moved the threshold down to $2m_t + 0.85$ GeV.

IV. CROSS SECTIONS AND ASYMMETRIES FOR $t\bar{t}$ NEAR THE Z

We are now in a position to put together the mixing formalism in Sec. II with the $t\bar{t}$ spectrum and wave functions of Sec. III. Indeed, for the ground state of $t\bar{t}$ we have already done this in that we explored the consequences of the mixing formalism by using it as an example in Sec. II for mass shifts, cross sections, and asymmetries in the two-state system consisting of the $1S$ state V_0 and the Z_0. Figures 10, 11, and 12 show the cross section in the neighborhood of the Z, for $e^+e^- \to \mu^+\mu^-$, normalized to $\sigma_{\rm pt} = 4\pi\alpha^2/3s$, for situations where $m_t = 45$, 47, and 49 GeV, respectively. In each case the distinct interference pattern of each of the 13 $^3S_1$ states assumed to be below open-top threshold is visible. As we move over the peak of the Z the peak-dip order in the interference changes to dip-peak.

The width (acquired by mixing) of the $t\bar{t}$ states decreases as we go to higher energy levels because the wave function at the origin (see Fig. 9) decreases, and so proportionally does the amplitude for mixing with the Z. However, the height of the peak (in R) remains approximately the same. In fact, the peaks of the V_0 resonances, as well as that of the Z_0, fall on a very slowly varying curve. This behavior is exactly correct for a resonance V

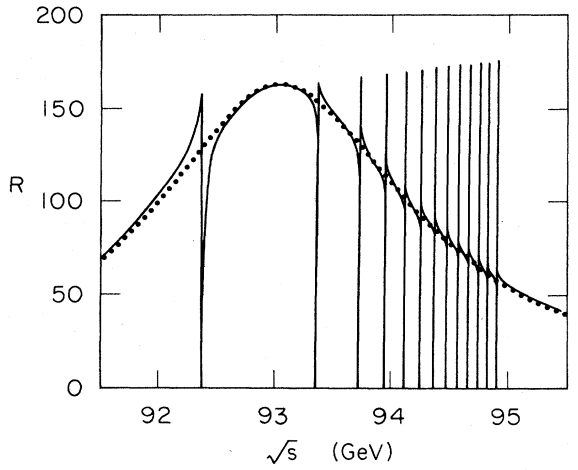

FIG. 11. $R(e^+e^- \to \mu^+\mu^-)$, including mixing of the Z with the first 13 $t\bar{t}$ states, for $m_t = 47$ GeV.

which acquires all its width from mixing with the Z, for from Eq. (2.19) we have

$$R = \frac{s^2(|g_{Z_0,L}|^2 + |g_{Z_0,R}|^2)_i(|g_{Z_0,L}|^2 + |g_{Z_0,R}|^2)_f}{64\pi^2\alpha^2 \left| s - M_{Z_0}^2 + i\Gamma_{Z_0}M_{Z_0} - \dfrac{(\delta m^2)^2}{s - M_{V_0}^2} \right|^2} . \tag{4.1}$$

This is a maximum for a value of s (very close to $M_{V_0}^2$) for which the real part of the quantity

$$(s - M_{Z_0}^2 + i\Gamma_{Z_0}M_{Z_0}) - \frac{(\delta m^2)^2}{s - M_{V_0}^2}$$

vanishes. At that point,

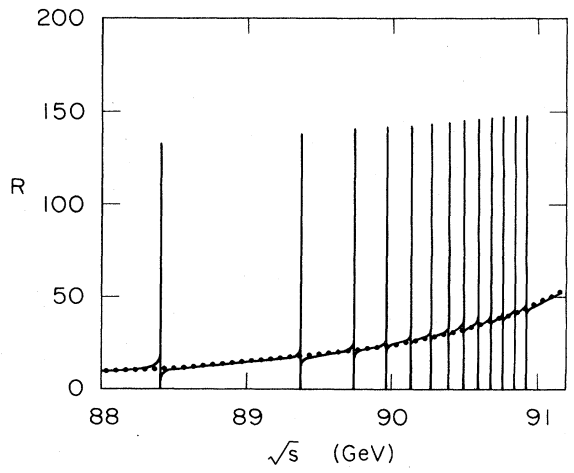

FIG. 10. $R(e^+e^- \to \mu^+\mu^-)$, including mixing of the Z with the first 13 $t\bar{t}$ states, for $m_t = 45$ GeV.

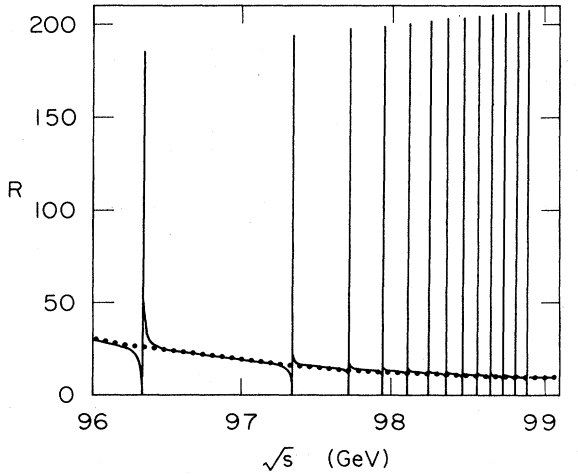

FIG. 12. $R(e^+e^- \to \mu^+\mu^-)$ including mixing of the Z with the first 13 $t\bar{t}$ states, for $m_t = 49$ GeV.

$$R_{\text{peak}} = \left[\frac{s_{\text{peak}}}{M_{Z_0}^2}\right]^2 \frac{M_{Z_0}^4(|g_{Z_0,L}|^2+|g_{Z_0,R}|^2)_i(|g_{Z_0,L}|^2+|g_{Z_0,R}|^2)_f}{64\pi^2\alpha^2|i\Gamma_{Z_0}M_{Z_0}|^2}$$
$$= \left[\frac{s_{\text{peak}}}{M_{Z_0}^2}\right]^2 R_{\text{peak},Z_0} \approx \left[\frac{M_V}{M_Z}\right]^4 R_{\text{peak},Z} \,. \tag{4.2}$$

Once we are above open-top threshold, the situation changes considerably. The width of an unmixed $t\bar{t}$ state presumably becomes tens of MeV, as is the case for the ψ'' and Υ'''. The peak and dip structure from interference with the Z is much less dramatic in $e^+e^-\to\mu^+\mu^-$, as is shown in Fig. 13. Here we have illustrated the situation by taking the 14^3S_1 state to be 2 GeV above the Z and to have a width of 20 MeV for decay into pairs of open-top states. The dashed curve shows the case of real δm^2 while the solid line indicates what happens when there is an imaginary part of the same magnitude (but opposite sign), which is a plausible possibility from Eq. (2.24). The imaginary part of δm^2 makes the interference pattern somewhat more impressive but when we note the suppressed zero for the vertical axis in Fig. 13 it is clear that in any case for $e^+e^-\to\mu^+\mu^-$ we have a much less impressive effect than that for a resonance below threshold. Of course, if we look at $e^+e^-\to t\bar{t}$, we will see a much greater effect, for $t\bar{t}$ is the major decay of such a resonance while $\mu^+\mu^-$ is a very minor one. However, once we are above open-top threshold the situation becomes quite complicated in that different states will mix with each other as well as the Z and the approximation inherent in producing zeros in the mass matrix in Eq. (2.23) breaks down. At the same time all the mixing matrix elements become complex. While interesting, a detailed investigation is beyond the scope of this paper.

The situation with respect to the polarization or front-back asymmetries when we include the whole spectrum of $^3S_1$ $t\bar{t}$ states is very much an iteration of what is found in Figs. 5, 6, and 7 for the $1S$ state. Of course, there are small variations as the t quark mass is changed and the "background" asymmetries due to the γ and Z change, but the general form of the interference pattern remains the same as we move over the peak of the Z. Again as we go to higher radial excitations, the width of the mixed $t\bar{t}$ states decreases (to $\lesssim 1$ MeV just below threshold) making the measurement of these large swings in the asymmetries very difficult.

This brings us to the question of how much of this is in fact measurable under actual experimental conditions where the spread in beam energy is not negligible. To see how this affects the results we have taken the curve in Fig. 11 (corresponding to $m_t=47$ GeV), which would be the measured cross section with no beam energy spread, and smeared it with a Gaussian corresponding to $\sigma_{E_{\text{beam}}}=40$ MeV (i.e., $\sigma_E/E\approx 0.8\times10^{-3}$) and to $\sigma_{E_{\text{beam}}}=100$ MeV (i.e., $\sigma_E/E\approx 2\times10^{-3}$). The results are shown by the solid and dashed curves, respectively, in Fig. 14. The latter case is currently the specification for the Stanford Linear Collider (SLC), although the former case, which is roughly nominal CERN LEP performance without wigglers, is also achievable[21] at SLC. In the latter case structure due to the higher $^3S_1$ states is washed out and we can only see a mild undulation due to the $1S$ state, instead of the deep dip in Fig. 4. In the former case, with a narrower beam spread, the ground state is quite clear

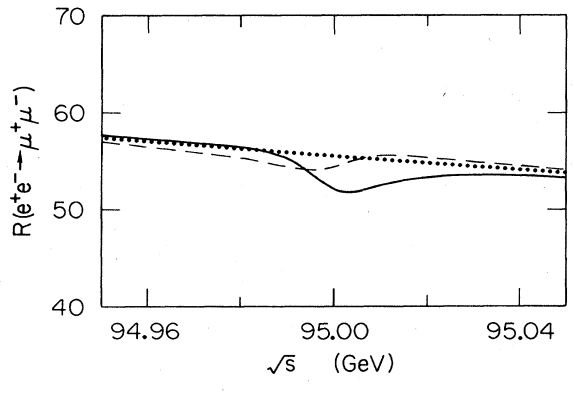

FIG. 13. $R(e^+e^-\to\mu^+\mu^-)$ for a $14S$ $t\bar{t}$ state with $M_{V_0}=95$ GeV/c^2 and $\Gamma_{V_0}=20$ MeV, and real δm^2 (dashed curve), and complex δm^2 with $\text{Im}\delta m^2/\text{Re}\delta m^2=-1$ (solid curve). The dotted curve is for the Z alone.

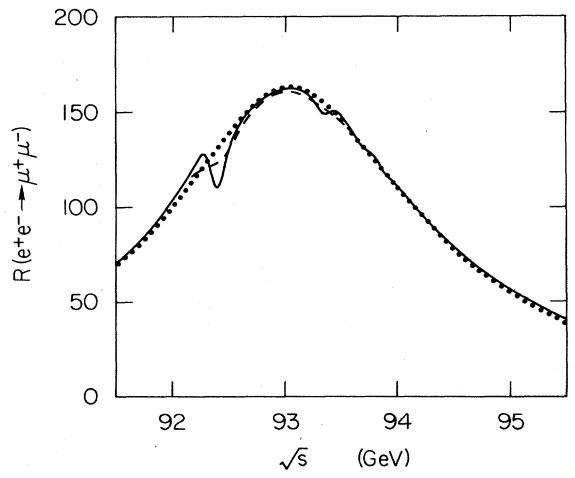

FIG. 14. The curve in Fig. 11, convoluted with a Gaussian appropriate for $\sigma_{\text{beam}}=40$ MeV (solid curve) and $\sigma_{\text{beam}}=100$ MeV (dashed curve). We show $R(e^+e^-\to\mu^+\mu^-)$ due to the Z alone (dotted curve) for comparison.

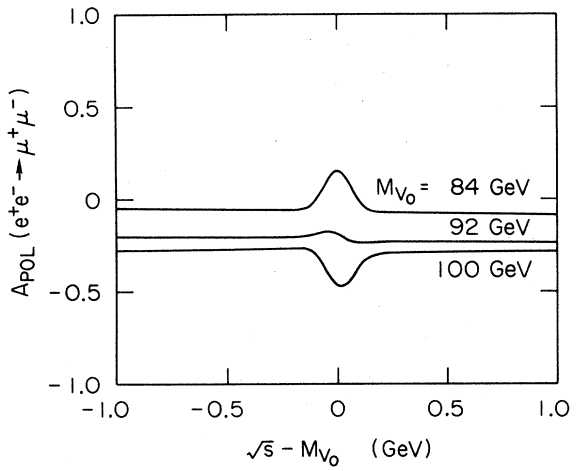

FIG. 15. The polarization asymmetry near the $1S$ $t\bar{t}$ state for $\sigma_{\text{beam}}=40$ MeV when $M_{V_0}=84$, 92, and 100 GeV.

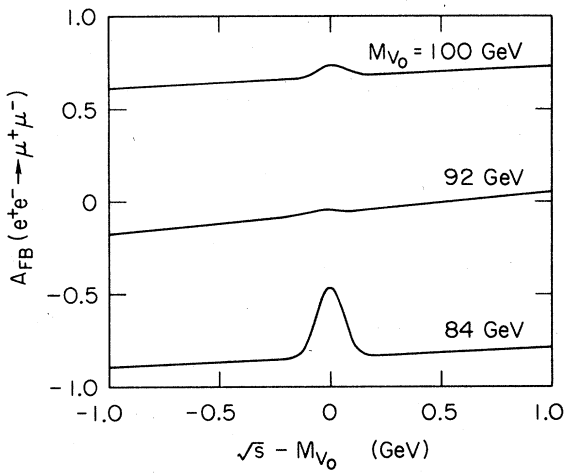

FIG. 16. The front-back asymmetry near the $1S$ $t\bar{t}$ state for $\sigma_{\text{beam}}=40$ MeV when $M_{V_0}=84$, 92, and 100 GeV.

and a few higher states can be picked off from their interference pattern with the Z.

The effects of smearing with $\sigma_{E_{\text{beam}}}=40$ MeV on A_{POL} and A_{FB} are shown for the ground state of $t\bar{t}$ in Figs. 15 and 16, respectively. Part of the reason these asymmetries have such a small variation when M_{V_0} is near M_Z (e.g., $M_{V_0}=92$ GeV in the figures), is that the unpolarized cross section due to the Z (which occurs in the denominator of the expression for the asymmetries) is large there. Even with the smearing one has fairly sizable effects in the asymmetries well below[22,23] or well above the Z.

Thus with $\sigma_{E_{\text{beam}}}\approx 40$ MeV one should be able to see quite distinctive indications for the first few levels of $t\bar{t}$ both in the cross section and the polarization and front-back asymmetries. Even with $\sigma_{E_{\text{beam}}}\approx 100$ MeV, if Nature is kind enough to put the $t\bar{t}$ state near the Z, the effects due to interference of the ground state with the Z are visible, and they are capable at least of giving us information on the properties of the t quark and, in particular, fairly precise knowledge of m_t and hence of where to look for the open-top threshold.

ACKNOWLEDGMENTS

We thank M. Peskin for suggestions and for the use of his program implementing the Richardson potential, and S. Güsken, J. H. Kühn, and P. Zerwas for communicating the results of their work before publication, as well as P. Zerwas for several discussions. One of us (P.J.F.) would also like to thank B. Ratra and J. Yeager for helpful suggestions. This work was supported by the U.S. Department of Energy, Contract No. DE-AC03-76SF00515.

[1]F. M. Renard, Z. Phys. C **1**, 225 (1979).

[2]L. M. Sehgal and P. M. Zerwas, Nucl. Phys. **B183**, 417 (1981). See also R. Budny, Phys. Rev. D **20**, 2763 (1979); and J. D. Jackson, S. L. Olsen, and S.-H. H. Tye, in *proceedings of the 1982 Summer Study on Elementary Particles and Fields, Snowmass, Colorado,* edited by R. Donaldson, R. Gustafson, and F. Paige (Fermilab, Batavia, Illinois, 1983), p. 175; L. M. Chang and J. N. Ng, TRIUMF report, 1984 (unpublished).

[3]W. Buchmüller, in *Proceedings of the Z^0 Theory Workshop, Ithaca, New York, 1981,* edited by M. E. Peskin and S.-H. H. Tye(Laboratory of Nuclear Studies, Cornell University Report No. CLNS 81-485), p. 210 and references therein; I. I. Y. Bigi and H. Krasemann, Z. Phys. C **7**, 127 (1981); J. H. Kühn, in *Electroweak Interactions,* proceedings of the 1982 Schladming School, Schladming, edited by H. Mitter (Springer, Vienna, 1982), p. 203; L. M. Sehgal, in *Electroweak Effects at High Energies,* proceedings of the 1983 Europhysics Study Conference, Erice, edited by H. D. Newman (Plenum, New York, in press); J. H. Kühn and S. Ono, Z. Phys. C **21**, 395 (1984); **24**, 404(E) (1984); J. H. Kühn, Acta Phys. Pol. **B12**, 347 (1981).

[4]E. Eichten, in *Proceedings of the 1984 SLAC Summer Institute on Particle Physics, Stanford,* edited by P. McDonough (SLAC, Stanford, in press).

[5]G. Arnison *et al.*, Phys. Lett. **126B**, 398 (1983); **135B**, 250 (1984); P. Bagnaia *et al.*, *ibid.* **129B**, 130 (1983).

[6]G. Arnison *et al.*, Phys. Lett. **147B**, 493 (1984).

[7]S. Güsken, J. H. Kühn, and P. M. Zerwas (in preparation). See also J. H. Kühn and P. M. Zerwas, CERN Report No. TH4089/85, 1985 (unpublished). Also, after submitting this paper for publication we received a report on similar work: L. J. Hall, S. F. King, and S. R. Sharpe, Harvard Report No. HUTP-85/A012, 1985 (unpublished).

[8]J. L. Richardson, Phys. Lett. **82B**, 272 (1979).

[9]S. Coleman and H. J. Schnitzer, Phys. Rev. **134**, 863 (1964).

[10]F. M. Renard, Springer Tracts Mod. Phys. **63**, 98 (1972); Y. Dothan and D. Horn, Nucl. Phys. **B114**, 400 (1976).

[11]Particle Data Group, Rev. Mod. Phys. **56**, S296 (1984).

[12]We thank M. Peskin for pointing out to us an explanation for the vanishing amplitude by noting that in the unmixed basis $\mathcal{M}_0^2-s\mathbf{1}$ has a zero for its V_0-V_0 element and consequently

$(\mathcal{M}_0^2 - s\mathbf{1})^{-1}$ has a zero for its Z_0-Z_0 element at $s = M_{V_0}^2 - iM_{V_0}\Gamma_{V_0}$. It is the latter matrix element that is picked off when the inverse propagator is sandwiched between coupling spinors when the V_0 has no coupling to either the initial or final fermions. We also thank P. Franzini and S. Drell for discussions leading to another explanation. The amplitude for $e^+e^- \to Z, V \to \mu^+\mu^-$ can be calculated by replacing the Z_0 propagator by the iterated series

$$\frac{1}{s - M_{Z_0}^2}\left[1 + \left[\frac{a}{s - M_{Z_0}^2}\frac{a}{s - M_{V_0}^2}\right] + \left[\ \right]^2 + \cdots\right] = \frac{s - M_{V_0}^2}{(s - M_{Z_0}^2)(s - M_{V_0}^2) - a^2},$$

which is zero for $s = M_{V_0}^2$.

[13]We take $M_Z = 93$ GeV for the remainder of the paper. All other masses are given relative to it, so that as a more exact value of the Z mass is measured, all our curves can be shifted appropriately. In addition we use $\sin^2\theta_W = 0.22$ and $\Gamma_Z = 2.7$ GeV (this does not include a contribution from the t quark); these values include the second-order electroweak corrections. However, in calculating our graphs for R we have implicitly cancelled a factor of $[\alpha(M_Z)]^2$ coming from the weak coupling of the Z against a factor of $[\alpha(0)]^2$ coming from the point cross-section. Therefore our curves for R should be increased by a factor of $[\alpha(M_Z)/\alpha(0)]^2 \approx 1.15$. We thank P. Zerwas for pointing out the discrepancy between Ref. 7 and our graphs.

[14]The t and $\bar{t}$ quarks in the $^3S_1$ $t\bar{t}$ states have a total width of ≈ 70 keV to decay weakly for $m_t = 45$ GeV, which is comparable to, or greater than, the combined width for such a state to decay by annihilation through photons or gluons, or to decay by a transition to another $t\bar{t}$ state. Hence, we take $\Gamma_{V_0} = 100$ keV for illustrative purpose.

[15]K. Gottfried, in *Proceedings of the 1981 International School of Nuclear Physics, Erice,* edited by D. Wilkinson (Pergamon, Oxford, 1982), p. 49. See also K. Gottfried, in *Proceedings of the International Europhysics Conference on High Energy Physics, Brighton, 1983,* edited by J. Guy and C. Costain (Rutherford Appleton Laboratory, Chilton, Didcot, United Kingdom, 1984), p. 747.

[16]We note that our levels, for the $1S$, $2S$, $3S$, $1P$, and $2P$ states, agree with those presented by Kühn and Ono (Ref. 3); see also Buchmüller (Ref. 3).

[17]R. Van Royen and V. Weisskopf, Nuovo Cimento **50**, 617 (1967).

[18]We have omitted QCD radiative corrections to Γ_{ee}; these would decrease the width by a factor of about 0.8.

[19]E. Eichten and K. Gottfried, Phys. Lett. **66B**, 286 (1977). See also C. Quigg and J. L. Rosner, *ibid.* **72B**, 462 (1978).

[20]J. Lee-Franzini, in *Proceedings of the 22nd International Conference on High Energy Physics, Leipzig, 1984,* edited by A. Meyer and E. Wieczore (Akademie der Wissenschaften der DDR, Zeuth, in press). See also K. Han *et al.*, Max Planck Report No. MPI-PAE/Exp-E1-148, 1985 (unpublished).

[21]R. Stiening (private communication).

[22]We thank P. Zerwas for pointing out the still sizable effects in asymmetries left after smearing when the $t\bar{t}$ state is well below the Z. See Ref. 7 for a detailed discussion.

[23]A. Martin, CERN Report No. TH4060/84, 1984 (unpublished).